Conference materials
UDC 53.082.52
DOI: https://doi.org/10.18721/JPM.161.222

Seasonal variations in optical attenuation spectra of some urban water bodies

V.S. Goryainov[1]✉, K.G. Antonenko[1], M. Khasenova[1], M.A. Malyga[1], I. A. Prosolov[1]

[1] St. Petersburg Electrotechnical University "LETI", St. Petersburg, Russia

✉ vsgoriainov@etu.ru

Abstract. Water samples were taken once a month from several urban water bodies, and using a laboratory setup with two concave mirrors and a fiber optic spectrometer attenuation spectra were obtained in visible and near infrared spectral range. Spectra approximation by a power law gave better fit, indicating the primary influence of scattering by non-algal particles on the total attenuation. Seasonal maximums of attenuation were observed in November and late in summer, attributed to detritus scatterings and algal bloom correspondingly. A negative correlation was found between the spectral slope parameter and the attenuation value at 550 nm, which means that spectra for more turbid samples were spectrally flatter in general.

Keywords: urban water bodies, minor water bodies, light attenuation spectra, seasonal variations_

Funding: The study was carried out as part of project FSEE-2020-0008, which was carried out as part of the state task of the Ministry of Science and Higher Education of the Russian Federation.

Citation: Goryainov V.S., Antonenko K.G., Khasenova M., Malyga M.A., Prosolov I.A., Seasonal variations in optical attenuation spectra of some urban water bodies, St. Petersburg State Polytechnical University Journal. Physics and Mathematics. 16 (1.2) 2023 146–152. DOI: https://doi.org/10.18721/JPM.161.222

Материалы конференции
УДК 53.082.52
DOI: https://doi.org/10.18721/JPM.161.222

Сезонные изменения оптических спектров ослабления в нескольких городских водоемах

В.С. Горяинов[1]✉, К.Г. Антоненко[1], М. Хасенова[1], М. А. Малыга[1], И.А. Просолов[1]

[1] Санкт-Петербургский государственный электротехнический университет «ЛЭТИ» им. В. И. Ульянова (Ленина), Санкт-Петербург, Россия

✉ vsgoriainov@etu.ru

Аннотация. Малые городские и пригородные водоемы являются важными объектами для регулярного экологического мониторинга, в том числе при помощи мониторинга их оптических свойств. В данном исследовании ежемесячно определялись спектры коэффициента ослабления излучения для нескольких водоемов при помощи оптоволоконного спектрометра и лабораторной установки с двумя вогнутыми зеркалами, установленными по бокам стеклянной кюветы. Наблюдалось различие в форме спектров между стоячими и проточными водоемами, а также резкое увеличение значений ослабления в стоячих водах в октябре и ноябре.

Ключевые слова: городские водоемы, малые водоемы, спектры ослабления света, сезонные изменения

Финансирование: Исследование проводилось в рамках проекта № FSEE0008-2020-, который выполнялся в рамках государственного задания Министерства науки и высшего образования Российской Федерации.

Ссылка при цитировании: Горяинов В.С., Антоненко К.Г., Хасенова М., Малыга М.А., Просолов И.А. Сезонные изменения оптических спектров ослабления в нескольких городских водоемах // Научно-технические ведомости СПбГПУ. Физико-математические науки. 2023. Т. 16. № 1.2. С. 146–152. DOI: https://doi.org/10.18721/JPM.161.222

Introduction

Minor urban and suburban water bodies are subject to a number of anthropogenic stress factors, including pollution by sewage waters, roadway runoff and pesticides, recreational load, as well as negative effects from redevelopment, draining and other artificial transformations. Slow water exchange makes such water bodies more prone to algal bloom and eutrophication as compared to natural waters [1]. All of the above increases the importance of regular ecological monitoring of urban and suburban water bodies.

Contemporary remote methods intended for studying natural waters rely mostly on the data obtained from spaceborne passive radiometers, spectrometers and hyperspectral cameras. However, the spatial resolution for most of such devices ranges from tens of meters to several kilometers [2, 3], which leaves out urban and suburban ponds, minor lakes, rivers and creeks. Consequently, other techniques are developed to study the properties of such water bodies, including the use of portable spectrometers [4] as well as sampling for subsequent hydro-optical measurements or chemical analysis [5].

In this study, spectra of the beam attenuation coefficient $c(\lambda)$, m^{-1} of water samples in the visible and near infrared (NIR) regions were measured. The attenuation coefficient is a principal hydro-optical parameter that describes the total attenuation of solar irradiation in the water and the consequent limitations on photosynthesis and green algae distribution. Using the spectra obtained, several problems were targeted by the study: (1) assessing the total turbidity of natural waters in question, (2) suggesting the optical phenomena that determine the shape of the spectra, (3) trying to distinguish between stagnant and flowing waters by their attenuation spectra, and (4) observing and analyzing the seasonal variations in the spectra.

Methods and Means of the Experiment

Objects of the study. The samples were taken once a month, from March to November 2021 altogether, from five water bodies in St. Petersburg, of which three were park ponds and two belonged to the Neva delta. Table 1 summarizes the sampling sites along with their latitude and longitude (obtained using GPS) and months (in Roman numerals) for which the samples were available.

Table 1

Sampling sites

Abbreviation	Water body	GPS coordinates	Months
BN	Bolshaya Nevka	59.97402, 30.32733	III, VI, IX – XI
RK	Karpovka	59.96752, 30.33002	IV, VI, IX – XI
IP	Iordanskiy pond	59.99366, 30.33595	VII – XI
SP	Serdobolskiy pond	59.99527, 30.33198	VII – XI
TsP	Tsvetochniy pond	59.99184, 30.34155	VII – XI

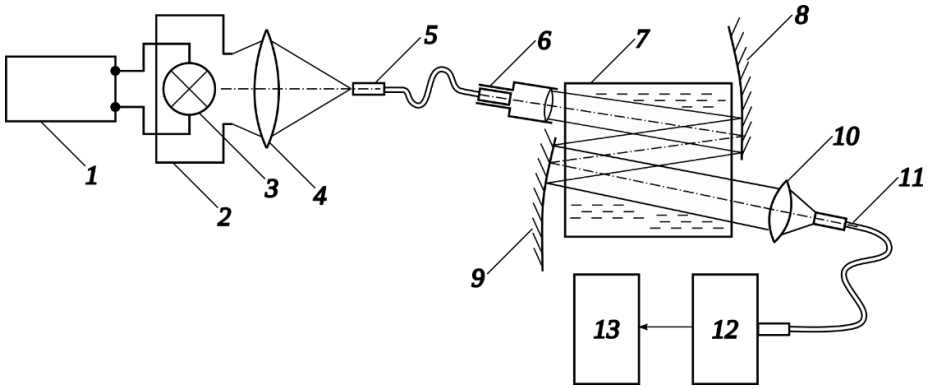

Fig. 1. Scheme of the laboratory setup: stabilized power supply *1*; opaque casing *2*; incandescent lamp *3*; converging lens *4*, *10*; fiber waveguide *5*, *11*; collimator *6*; glass cuvette *7*; concave mirror; *12* — fiber optic spectrometer *8*, *9*; computer *13*

The laboratory setup. The setup used for laboratory measurements relied on the well-known idea of extending the path traveled by light in water (Fig. 1). For this purpose, two concave mirrors *8* and *9* were installed on both sides of a 50 mm glass cuvette *7*. Earlier version of the setup used a concave mirror and a plane one, with light passing through the cuvette twice [6]. Some attempts at measuring scattering were also made using that setup, but then the current one was introduced, in which light passes through the cuvette three times, in order to highlight the spectral features more clearly.

The fiber optic spectrometer used for the measurements was an Ocean Insight's USB650 Red Tide. Its crossed Czerny-Turner optical design provided spectral resolution of 2 nm FWHM in the wavelength range from 350 to 1000 nm. The integration time was generally from 10 to 100 ms depending on the sample's turbidity.

For every sample, the following sequence of measurements was performed. First the cuvette was filled with distilled water, and after the necessary adjustments, the spectral intensity distribution ($I_0(\lambda) - I_{D1}(\lambda)$) was registered, with $I_{D1}(\lambda)$ being the noise spectrum (spectrometer's CCD dark current) recorded with the lamp shut off, stored and subtracted internally by the spectrometer's control software. After that, the cuvette was filled with water from the sample under study, the integration time was adjusted if necessary, and the second intensity distribution ($I_T(\lambda) - I_{D2}(\lambda)$) was recorded. In case of very clear sample, both spectra could be recorded using the same integration time, with $I_{D1}(\lambda) = I_{D2}(\lambda)$, obviously. Every measurement was repeated 20 times to enable averaging and estimating the accuracy.

Processing the experimental data. Using the aforementioned data, the attenuation coefficient spectrum was calculated by the following formula:

$$c(\lambda) = \frac{1}{3d} \ln\left[\frac{I_0(\lambda) - I_{D1}(\lambda)}{I_T(\lambda) - I_{D2}(\lambda)}\right], \tag{1}$$

where d is the cuvette length.

To approximate the spectrum's shape, two models were used: a decreasing exponent [7]:

$$c_e(\lambda) = c_e(\lambda_0)\exp\left[-S_e\left(\lambda - \lambda_0\right)\right], \tag{2}$$

and a decreasing power function [8]:

$$c_p(\lambda) = c_p(\lambda_0)\left[\lambda / \lambda_0\right]^{-S_p}, \tag{3}$$

where λ_0 is a reference wavelength and S_e, S_p are the spectral slope parameters.

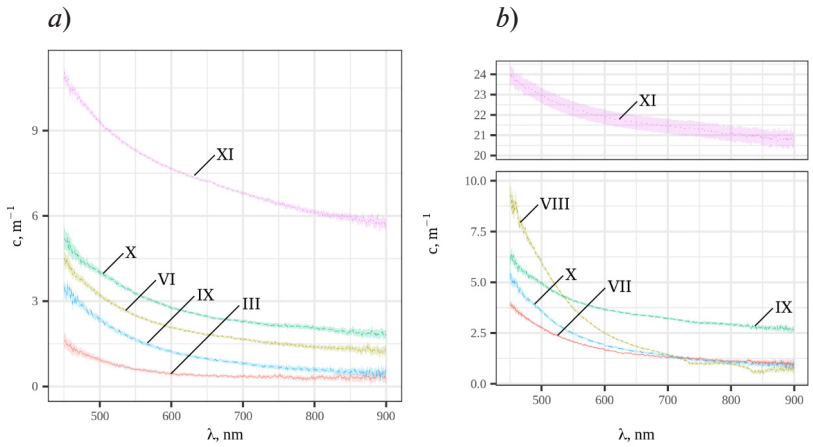

Fig. 2. Attenuation spectra for two water bodies: BN (flowing) (*a*), SP (stagnant) (*b*). Roman numerals denote months. The vertical axis in plot (*b*) is broken due to high attenuation values in November

Since both models are based on a nonlinear function, instead of the coefficient of determination R^2, the Bayesian information criterion (BIC) was used to estimate the quality of approximation [9]:

$$BIC = k\ln(n) - 2\ln\left(\hat{L}\right), \tag{4}$$

where $\hat{L}$ is the maximized likelihood of the model, n the number of points in a spectrum, and $k = 1$ is the number of parameters estimated by the model.

All the calculations were performed using the R language and software for statistical computing [10–12].

Results

As an example of obtained results, Fig. 2 shows the averaged attenuation spectra for two of the water bodies, representing both running waters (BN) and stagnant ones (SP), with Roman numerals denoting months. Semitransparent ribbons along the plot lines show the standard deviation σ.

The power function model (3) gave overall lower BIC values, indicating better fit. Fig. 3 shows the seasonal variations of the spectral slope parameter S_p obtained from approximation (*a*), and of the attenuation coefficient value at 550 nm $c(550)$ (*b*).

Due to relatively low color temperature of the halogen incandescent lamp used as a source of radiation, only the spectral range from 450 to 900 nm was taken into account during approximation. Table 2 contains the Bayesian information criterion (4) values averaged over all the corresponding spectra for each of the water bodies.

Table 2

Comparison of average BIC values for the two approximation models

Water body	Exponential	Power
BN	239.66	–130.69
RK	553.87	139.43
IP	435.73	–367.36
SP	613.60	4.96
TsP	1152.53	141.63

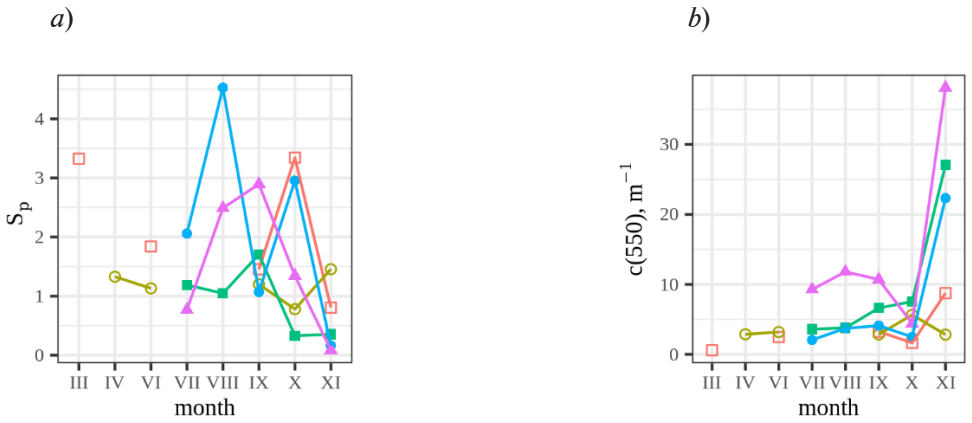

Fig. 3. Seasonal dependence of the spectral slope parameter S_p (*a*) and of the attenuation coefficient value at 550 nm (*b*). The symbols denote the water bodies: □ corresponds to BN, ○ corresponds to RK, ■ corresponds to IP, ● corresponds to SP, ▲ corresponds to TsP

To consider the possible correlation between S_p and $c(550)$, a scatter plot of the two parameters is presented in Fig. 4. Disregarding the separation by water body, Spearman rank correlation coefficient was $\rho = -0.62$. Separate calculations for each of the water bodies gave ρ of -0.9 for BN and RK, -0.6 for IP and SP, and -0.2 for TsP. In other words, higher $c(550)$ values (more turbid samples) corresponded to slower decrease of attenuation with wavelength increasing, and to flatter spectra.

Discussion

All the spectra obtained in the study showed attenuation decreasing from the blue region to NIR. The models considered for spectral approximation describe absorption of radiation by detritus and non-algal particles [7], and scattering by the same components [8]. With the second model fitting better to experimental data, scattering by detritus might be suggested as the primary process determining the spectra shape. The authors in [8] give an average spectral slope parameter $S_p = 0.938$, which is comparable to the values obtained for RK, or IP and TsP in midsummer months.

The samples from flowing waters (BN and RK) were generally clearer, resulting in lower attenuation values, as Fig. 3,*b*, and the distribution of points along the horizontal axis in Fig. 4 show. The spectral slope parameter, on the other hand, varied more or less widely for all the water bodies, so from the data available, no universal rule can be produced to distinguish between stagnant and flowing waters by the shape of their attenuation spectra. However the two classes of waters showed different seasonal patterns in S_p and c(550) values.

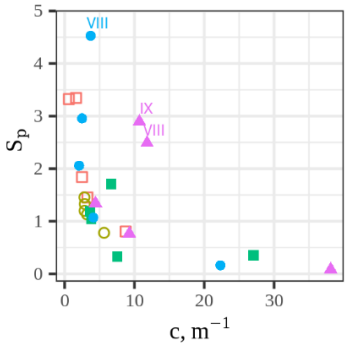

Fig. 4. Interrelation between the spectral slope parameter and the attenuation coefficient value at 550 nm. The symbols denote the water bodies: □ corresponds to BN, ○ corresponds to RK, ■ corresponds to IP, ● corresponds to SP, ▲ corresponds to TsP. Some notable points are marked by Roman numerals denoting months.

The absolute attenuation maximums for all the water bodies except RK were observed in November (Fig. 3,*b*). The corresponding samples were taken from under the ice edge, near the bank, and appeared visually as very turbid suspension of detritus and mineral particles. The high random error in measurements of attenuation (a wide ribbon along the XI line in Fig. 2, *b*) can be attributed to sedimentation of suspended matter during the measurement reducing turbidity of the sample.

Another maximums for the stagnant waters were observed in late summer (lack of data for flowing waters prevents the comparison between the two classes of water bodies). Rising and decreasing attenuation can be seen for TsP and less prominently, for SP (Fig. 3, *b*). In addition, these points do not follow the general negative correlation between $c(550)$ and S_p stated at the end of the Results section, and appear as outliers with respect to the main trend in Fig. 4, marked with Roman numerals. Such results can be attributed to algae blooming in these two ponds. In the third pond (IP), the same effect appeared in September and to a lesser extent.

Several study limitations arise from its design and conditions. Firstly, comparing the spectra obtained to some results of hydrochemical analysis of the samples could have been very valuable.

Secondly, minor water bodies are prone to rapid ecological changes due to relatively small water mass. For example, chlorophyll concentration in a small pond can follow not only seasonal changes in solar irradiance, but also weather changes and time of day. Studying such processes requires frequent sampling which can be time-consuming, or using submersible probes capable of autonomous operation [13].

REFERENCES

1. **Bondarenko E.A., Starkov V.A., Andrianova M.Ju.**, Fluorimetric tracing of sewage effluents in the Murinsky creek, Construction of Unique Buildings and Structures. 9 (24) (2014) 27–38.

2. **Krueger J.K., Selva D., Smith M.W., Keesee J.**, Spacecraft and constellation design for a continuous responsive imaging system in space, In: AIAA SPACE 2009 Conference & Exposition, Pasadena, USA, 2009. 6773.

3. **Zhu L., Suomalainen J., Liu J., Hyyppa J., Kaartinen H., Haggren H.**, A review: remote sensing sensors, In: Multi-purposeful Application of Geospatial Data, IntechOpen, London, 2017. 71049.

4. **Liang Q., Zhang Y., Ma R, Loiselle S., Li J., Hu M.**, A MODIS-based novel method to distinguish surface cyanobacterial scums and aquatic macrophytes in lake Taihu, Remote Sensing. 2 (9) (2017) 133.

5. **Andrianova M.J., Bondarenko E.A., Krotova E.O., Chusov A.N.**, Comparison of chemical and optical parameters in monitoring of urban river Okhta, In: EESMS 2014 – 2014 IEEE Workshop on Environmental, Energy and Structural Monitoring Systems, Proceedings. 2014. 198–202.

6. **Горяинов В.С., Хасенова М., Антоненко К.Г., Бузников А.А.**, Лабораторный измеритель гидрооптических характеристик на основе волоконно-оптического спектрометра, Известия СПбГЭТУ «ЛЭТИ». 2 (2021) 5–14.

7. **Bricaud A., Morel A., Babin M., Allali K., Claustre H.**, Variations of light absorption by suspended particles with chlorophyll a concentration in oceanic (case 1) waters: analysis and implications for bio-optical models, Journal of Geophysical Research. C13 (103) (1998) 31033–31044.

8. **Sun D., Li Y., Wang Q., Lv H., Le C., Huang C., Gong S.**, Partitioning particulate scattering and absorption into contributions of phytoplankton and non-algal particles in winter in Lake Taihu (China), Hydrobiologia. 644 (2010) 337–349.

9. **Spiess A.-N., Neumeyer N.**, An evaluation of R^2 as an inadequate measure for nonlinear models in pharmacological and biochemical research: a Monte Carlo approach, BMC Pharmacology. 10 (2010) 6.

10. **R Core Team**, R: A Language and Environment for Statistical Computing, R Foundation for Statistical Computing, Vienna, 2020.

11. **Wickham H.**, ggplot2: Elegant Graphics for Data Analysis. Springer-Verlag, New York, 2016.

12. **Xu S., Chen M., Feng T., Zhan L., Zhou L., Yu G.,** Use ggbreak to effectively utilize plotting space to deal with large datasets and outliers, Frontiers in Genetics. 12 (2021) 774846.

13. **Leeuw T., Boss E.S., Wright D.L.**, In situ measurements of phytoplankton fluorescence using low cost electronics, Sensors. 6 (13) (2013) 7872–7883.

THE AUTHORS

GORYAINOV Viktor S.
vsgoriainov@etu.ru
ORCID: 0000-0003-2864-8717

ANTONENKO Kseniya G.
kgantonenko@yandex.ru
ORCID: 0000-0002-5776-877X

KHASENOVA Mariyam
mariyam-98@mail.ru
ORCID: 0000-0002-9352-7121

MALYGA Mikhail A.
mmalyga@list.ru
ORCID: 0000-0003-1844-4104

PROSOLOV Igor A.
prosolovigor@gmail.com
ORCID: 0000-0002-9443-7427

Received 09.11.2022. Approved after reviewing 15.11.2022. Accepted 17.11.2022.